Orthonormal Vector Sets Regularization with PDE's and Applications

DAVID TSCHUMPERLÉ AND RACHID DERICHE
Odyssee Lab, I.N.R.I.A Sophia Antipolis, 06902 Sophia Antipolis, France
David.Tschumperle@sophia.inria.fr
Rachid.Deriche@sophia.inria.fr

Abstract. We are interested in regularizing fields of *orthonormal vector sets*, using constraint-preserving anisotropic diffusion PDE's. Each point of such a field is defined by multiple orthogonal and unitary vectors and can indeed represent a lot of interesting *orientation features* such as direction vectors or orthogonal matrices (among other examples). We first develop a general variational framework that solves this regularization problem, thanks to a constrained minimization of ϕ-functionals. This leads to a set of coupled vector-valued PDE's preserving the orthonormal constraints. Then, we focus on particular applications of this general framework, including the restoration of noisy direction fields, noisy chromaticity color images, estimated camera motions and DT-MRI (Diffusion Tensor MRI) datasets.

Keywords: partial differential equations (PDE), constrained vector-valued regularization, orientation features, anisotropic diffusion, orthogonal matrices

1. Introduction

In the last decade, the restoration of noisy and blurred digital data has attracted a growing interest and many computer algorithms, based on variational or stochastic formulations have tried to solve this ill-posed inverse problem. The variational methods based on functional minimization via *diffusion PDE's* have particularly proven their efficiencies in order to regularize images while preserving important global structures, such as object contours (that are discontinuities in the measured signal). Actually, one of the first step has been crossed ten years ago, with the pioneering work of Perona and Malik (1990), who proposed an anisotropic diffusion PDE allowing to smooth grey-valued images while preserving edges, breaking then the limitations of classic linear filtering techniques. Since then, many authors have proposed and studied well-posedness PDE's that tackle the problem of scalar image regularization (particularly within the ϕ-function framework). We can cite for instance reference papers from Alvarez

et al. (1992), Charbonnier et al. (1994), Chambolle and Lions (1997), Strong and Chan (1996a, 1996b), Cohen (1995), Cottet and Germain (1993), Kornprobst et al. (1997a, 1997b, 1998), Malladi and Sethian (1996), Mumford and Shah (1989), Shah (1996), Morel and Solimini (1988), Nordström (1990), Osher and Rudin (1994), Proesmans et al. (1994), Caselles et al. (1998), Sapiro (2001), Weickert (1997, 1998), and You et al. (1994).

More recently and thanks to the increase of computer performances, the problem of addressing noisy multivalued datasets has opened a large and active research area, due to the high number of possible applications including various computer vision tasks, such as color image restoration (Blomgren and Chan, 1998; Kimmel et al., 2000; Sapiro and Ringach, 1996; Sochen et al., 1997; Sternberg, 1991; Tschumperlé and Deriche, 2001a; Weickert, 1998) and segmentation (Chan et al., 2000; Koschan, 1995; Paragios and Deriche, 2002; Sapiro, 1996, 1997), regularization of optical flows and direction fields (Bertalmio et al.,

2001; Chan and Shen, 2001a; Kimmel and Sochen, 2002; Nagel and Enkelmann, 1986; Perona, 1998; Tang et al., 2000; Tschumperlé and Deriche, 2001c; Vese and Osher, 2002) , image in-painting (Bertalmio et al., 2000; Chan and Shen, 2000, 2001b), scale space analysis (Alvarez et al., 2002; Weickert, 1999), etc. A PDE flow on multi-valued data is not a straightforward generalization of its scalar counterpart, since it must explicitly take the coupling between vector components as well as the local vector geometry into account. Indeed, the vector data may lie on *a constrained and non-flat manifold*, and new theoretical developments are involved. This generally yields to significant modifications of the corresponding evolution equations by adding coupling terms that allow the constraint to be preserved along the PDE flow.

For instance, this is the case when one wants to restore fields of unitary vectors, that lie on the unit sphere S^n (Chan and Shen, 2001a; Kimmel and Sochen, 2002; Perona, 1998; Tang et al., 2000; Vese and Osher, 2002) or on manifolds implicitly defined by level sets functions (Bertalmio et al., 2001).

Following these previous works, the aim of this article is to propose a variational framework, allowing to regularize an original type of constrained vector data: fields of *n-D orthonormal vector sets*. Indeed, many interesting informations can be represented by such datasets. We find of course the expected case of the unit sphere S^n, when the orthonormal sets are reduced to single vectors. But it can also represent more complex manifolds such as $O(n)$, the space of orthogonal matrices. Actually, the orthonormal vector sets are well adapted to represent *orientation features*, such as direction vectors, chromaticity features in color images, rotation matrices or diffusion tensor orientations. The idea is then to find a common variational formulation that allows to diffuse directly such structures with vector-valued PDE's, avoiding any reparametrization step (the case of 3D rotations, decomposed in Euler angles or unit quaternions will be discussed and illustrated in Section 6.1).

The paper is organized as follows: We first propose a mathematical formulation of the orthonormal vector sets regularization problem (Section 2), then propose a diffusion PDE-based solution, coming from the constrained gradient descent of a ϕ-functional minimization (Section 3). The role of the orthonormal constraints will be discussed and particular cases will be illustrated: In a first part, we are interested in the simple case where each image feature is a unitary n-D vector

belonging to the unit sphere S^n. This allows us to draw a direct parallel with previous works on direction diffusion (Chan and Shen, 2001a; Kimmel and Sochen, 2002; Perona, 1998; Tang et al., 2000; Tschumperlé and Deriche, 2001a; Vese and Osher, 2002) (Section 4). Then, we go one step further by studying the particular case of 3×3 orthogonal matrices which also fits our proposed framework (Section 5). The derived equations are interpreted through a mechanical viewpoint and suitable numerical schemes are then provided.

Many applications of interest can benefit from this regularization framework. We will illustrate both particular cases of direction vectors and orthogonal matrices studied in this paper with applications to the regularization of direction fields (coming from instance from optical flows computation) and color images with chromaticity noise (as proposed in Chan and Shen (2001a), Kimmel and Sochen (2002), Perona (1998), Tang et al. (2000), Tschumperlé and Deriche (2001a), and Vese and Osher (2002)). We also address two original and challenging problems: First, the restoration of noisy camera motion estimations, allowing smooth re-projections of 3D virtual objects in real movies (Section 6.1). Then, the regularization of DT-MRI datasets (diffusion tensor MRI (Coulon et al., 2001a, 2001b; Le Bihan, 2000; Poupon et al., 1998; Vemuri et al., 2001)), leading to the construction of coherent tissues fibers maps in the white matter of the brain (Section 6.2). Experimental results are finally presented in the end of this paper (Section 7).

2.   Notations and Context

Vector-valued variables will be referred to by bold letters. Let us consider m vector-valued images

$$\mathbf{I}^{[k]} : \Omega \to \mathbb{R}^n \quad (1 \leq k \leq m, n \in \mathbb{N}^+)$$

supposed twice differentiable on a subset Ω of $\mathbb{R}^p$ (usually $p = 1, 2$ or 3). We will denote by

$$I_i^{[k]} : \Omega \to \mathbb{R} \quad (1 \leq k \leq m, 1 \leq i \leq n)$$

the scalar image, corresponding to the ith vector component of $\mathbf{I}^{[k]}$. Then, $\forall \mathbf{x} \in \Omega$,

$$\mathbf{I}^{[k]}(\mathbf{x}) = \left(I_1^{[k]}(\mathbf{x}), I_2^{[k]}(\mathbf{x}), \ldots, I_n^{[k]}(\mathbf{x}) \right)^{\mathrm{T}}$$

We are particularly interested in the set

$$\mathcal{B} = \left\{ \mathbf{I}^{[k]} \,\middle|\, 1 \le k \le m \right\}$$

of the m vector-valued images $\mathbf{I}^{[k]}$. It can be seen itself as a field, where each point is a *vector set*:

$$\forall \mathbf{x} \in \Omega, \quad \mathcal{B}(\mathbf{x}) = \left\{ \mathbf{I}^{[1]}(\mathbf{x}), \mathbf{I}^{[2]}(\mathbf{x}), \dots, \mathbf{I}^{[m]}(\mathbf{x}) \right\}$$

Suppose now that the following *orthonormal constraints* between the vectors $\mathbf{I}^{[k]}$ are also verified:

$$\forall \mathbf{x} \in \Omega, \quad \mathbf{I}^{[k]}(\mathbf{x}) \cdot \mathbf{I}^{[l]}(\mathbf{x}) = \delta_{kl} = \begin{cases} 1 & \text{if } k = l \\ 0 & \text{if } k \ne l \end{cases} \quad (1)$$

where $\mathbf{I}^{[k]}(\mathbf{x}) \cdot \mathbf{I}^{[l]}(\mathbf{x}) = \sum_{i=1}^{n} I_i^{[k]}(\mathbf{x}) \, I_i^{[l]}(\mathbf{x})$ is the usual dot product in $\mathbb{R}^n$. Then,

$$\forall \mathbf{x} \in \Omega, \quad \mathcal{B}(\mathbf{x}) \text{ is an orthonormal vector set}$$

composed of m orthogonal and unit vectors of dimension n. Note that one particularly interesting case is reached when $m = n$, then $\mathcal{B}$ is *an orthonormal vector basis* in $\mathbb{R}^n$.

In this paper, we propose a general way to regularize any datasets that can be modeled as a field $\mathcal{B}$ of orthonormal vector sets, using coupled anisotropic diffusion PDE's. This idea is motivated by the fact that orthonormal vector sets are well designed to represent *data orientation features*, including:

- *Unitary vectors*: When the set $\mathcal{B}$ is restricted to a single vector image $\mathcal{B} = \{\mathbf{I}\}$ (i.e. $m = 1$), the orthonormal constraints (1) reduce to

$$\forall \mathbf{x} \in \Omega, \quad \|\mathbf{I}(\mathbf{x})\| = 1$$

which characterizes fields of unitary vectors (Fig. 1(a)).
- Orthogonal matrices: The columns of an orthogonal matrix $\mathcal{R} \in O(n)$ are unit vectors that form an orthonormal vector basis. Then, $\mathcal{R}$ can be equivalently represented by an orthonormal vector set $\mathcal{B}$ (with $m = n$, the matrix dimension) (Fig. 1(b)). Note that $O(n)$ is a kind of bi-dimensional extension of S^n, and have the same non-flat vector structure (due to the orthonormal constraints).

These two particular cases will be more particularly studied in Sections 4 and 5. First of all, let us develop
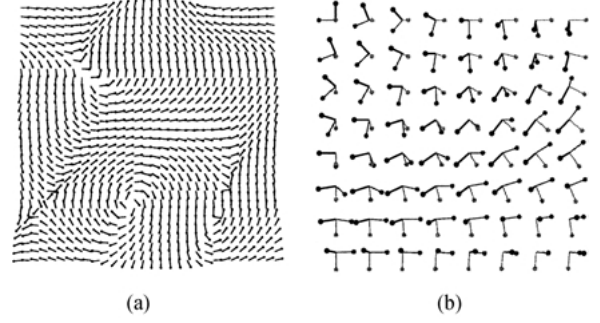

Figure 1. Examples of 2D fields of orthogonal vector sets ($p = 2$). (a) Field of 2D Direction vectors ($m = 1$, $n = 2$). (b) Field of 3D Orthogonal matrices ($m = 3$, $n = 3$).

a variational formulation to address the case of general orthonormal vector sets ($m, n \in \mathbb{N}^+$).

3. A Variational Formulation

We consider an initial "noisy" image $\mathcal{B}_0$ of *orthonormal vector sets* (verifying constraints (1))

$$\forall \mathbf{x} \in \Omega, \quad \mathcal{B}_0(\mathbf{x}) = \left\{ \mathbf{I}^{[1]}(\mathbf{x})_0, \mathbf{I}^{[2]}(\mathbf{x})_0, \dots, \mathbf{I}^{[m]}(\mathbf{x})_0 \right\}$$

that we want to regularize using variational flows preserving the orthonormal structure of these vector sets (Fig. 2).

3.1. Unconstrained Regularization

We propose to find $\mathcal{B}$ as the solution of an energy minimization, following the well know idea of ϕ-function diffusion, used to restore scalar images (see for instance Charbonnier et al. (1994), Kornprobst et al. (1997b, 1998), and Perona and Malik (1990)), and more recently, vector fields (Blomgren and Chan, 1998; Kimmel et al., 2000; Sochen et al., 1997). We quickly remind the idea: Each vector image $\mathbf{I}_0^{[k]}$ of the set $\mathcal{B}_0$ can
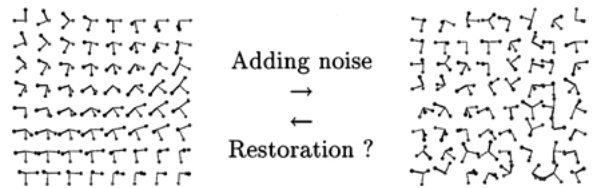

Figure 2. How to regularize a field $\mathcal{B}$ of orthonormal vector sets?

be anisotropically smoothed (denoising with preservation of discontinuities), by minimizing the following ϕ-functional

$$E\big(\mathbf{I}^{[k]}\big) = \int_{\Omega} \left(\frac{\alpha}{2} \big\| \mathbf{I}^{[k]} - \mathbf{I}_0^{[k]} \big\|^2 + \phi\big(\big\| \nabla \mathbf{I}^{[k]} \big\| \big) \right) d\Omega$$

(2)

where $\| \nabla \mathbf{I}^{[k]} \| = \sqrt{\sum_{i=1}^{n} \| \nabla I_i^{[k]} \|^2}$ is defined as the *vector gradient norm* and measures a global vector variation both in norm and orientation. The fixed parameter $\alpha \in \mathbb{R}$ prevents the final solution from being too different from the initial given field $\mathbf{I}_0^{[k]}$. The function $\phi : \mathbb{R} \rightarrow \mathbb{R}$ is a *diffusion function*, which controls the regularization behavior. A lot of different ϕ-functions have already been proposed in the literature related to scalar image restoration: Minimal surfaces (Charbonnier et al., 1994) Geman and McClure (1985), Perona and Malik (1990), Total variation (Rudin et al., 1992), Tikhonov (1963) (choosing the right ϕ-function depends on the desired regularization behavior, we refer the interested reader to Charbonnier et al. (1994) and Kornprobst et al. (1997b, 1998)).

One way of minimizing the functional $E(\mathbf{I}^{[k]})$, is to compute the corresponding *vector Lagrangian* $\mathcal{L}^{[k]} \in \mathbb{R}^n$ which is in this case (using a component by component writing style):

$$\mathcal{L}_i^{[k]} = \alpha\big(I_i^{[k]} - I_{i_0}^{[k]} \big) - \mathrm{div}\left(\frac{\phi'\big(\| \nabla \mathbf{I}^{[k]} \| \big)}{\| \nabla \mathbf{I}^{[k]} \|} \nabla I_i^{[k]} \right)$$

Then, one uses m vector gradient descents until steady state: $\frac{\partial \mathbf{I}^{[k]}}{\partial t} = -\mathcal{L}^{[k]}$, i.e. the $m \times n$ following scalar PDE's:

$$\begin{cases} \mathbf{I}_{(t=0)}^{[k]} = \mathbf{I}_0^{[k]} \\ \frac{\partial I_i^{[k]}}{\partial t} = \alpha\big(I_{i_0}^{[k]} - I_i^{[k]} \big) + \mathrm{div}\left(\frac{\phi'\big(\| \nabla \mathbf{I}^{[k]} \| \big)}{\| \nabla \mathbf{I}^{[k]} \|} \nabla I_i^{[k]} \right) \end{cases}$$

$(1 \leq i \leq n$ and $1 \leq k \leq m)$.   (3)

For our purpose of orthonormal vector set regularization, one could naively use such diffusion PDE's (3) on each vector $\mathbf{I}_0^{[k]}$ of the orthonormal vector set $\mathcal{B}_0$, then reconstruct the final vector set image $\mathcal{B}$ with the resulting smoothed vectors. A result of this method is illustrated on Fig. 3. Two regularizing PDE's (3) were applied on each vector of 2D orthonormal vector bases $\mathcal{B} = \{\mathbf{I}^{[1]}, \mathbf{I}^{[2]}\}$ (mixture of direct and indirect bases), using the Tikhonov function $\phi(s) = s^2$.
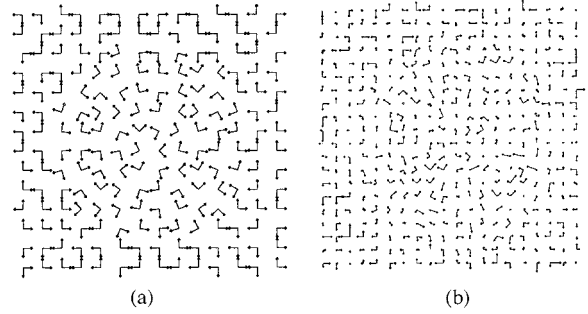

Figure 3. Decoupled diffusion of orthonormal vector sets: Orthonormal constraints are broken. (a) Original test field $\mathcal{B}_0$. (b) "Regularized" field $\mathcal{B}$ with (3).

Unfortunately, this decoupled regularization method breaks the orthonormal properties: vector norms and orthogonal angles are not intrinsically preserved by (3). We must explicitly introduce *orthonormal constraints*, in the minimization process. Note that conversely to regularization methods acting on S^n that led to PDE's with coupling terms between vector components, our problem is more general since the equations must also consider an additional orthogonal coupling between the different vectors themselves.

3.2. *A Way of Preserving the Orthonormal Constraints*

In order to regularize the field of orthonormal vector sets $\mathcal{B}_0$ while preserving the orthonormal properties (1), we propose a constrained minimization of the following functional:

$$E(\mathcal{B}) = \sum_{k=1}^{m} E\big(\mathbf{I}^{[k]}\big)$$

which also writes:

$$E(\mathcal{B}) = \int_{\Omega} \sum_{k=1}^{m} \left(\frac{\alpha}{2} \big\| \mathbf{I}^{[k]} - \mathbf{I}_0^{[k]} \big\|^2 + \phi\big(\big\| \nabla \mathbf{I}^{[k]} \big\| \big) \right) d\Omega$$

(4)

with respect to the m vector images $\mathbf{I}^{[k]}$, *subject to the orthonormal constraints*:

$$\forall \mathbf{x} \in \Omega, \quad \mathbf{I}^{[p]}(\mathbf{x}) \cdot \mathbf{I}^{[q]}(\mathbf{x}) = \delta_{pq} = \begin{cases} 1 & \text{if } p = q \\ 0 & \text{if } p \neq q \end{cases}$$

(1)

Note that the m Lagrangian vectors $\mathcal{L}^{[k]}$ of the energy

$E(\mathcal{B})$ are obviously the same than in Section 3.1, i.e

$$\mathcal{L}_i^{[k]} = \alpha\big(I_i^{[k]} - I_{i_0}^{[k]}\big) - \operatorname{div}\left(\frac{\phi'\big(\big\|\nabla\mathbf{I}^{[k]}\big\|\big)}{\big\|\nabla\mathbf{I}^{[k]}\big\|}\nabla I_i^{[k]}\right)$$

It is then equivalent to associate at each vector $\mathbf{I}^{[k]}$ an energy functional $E(\mathbf{I}^{[k]})$ as defined in (2).

The orthonormal constraints are then introduced by adding m^2 Lagrange multipliers λ_{pq}: $\Omega \to \mathbb{R}$ (where $p, q \in [1, m]$) to the functional $E(\mathcal{B})$, where each λ_{pq} is associated with the constraint:

$$\forall \mathbf{x} \in \Omega, \quad \mathbf{I}^{[p]}(\mathbf{x}) \cdot \mathbf{I}^{[q]}(\mathbf{x}) = \delta_{pq}$$

It leads to the *unconstrained minimization* of the following functional, with respect to $\mathbf{I}^{[k]}$ and λ_{pq}:

$$E^*(\mathcal{B}, \lambda)$$
$$= E(\mathcal{B}) + \int_\Omega \sum_{(p,q)\in[1,m]} \lambda_{pq}\big(\mathbf{I}^{[p]} \cdot \mathbf{I}^{[q]} - \delta_{pq}\big)\, d\Omega$$

In fact, as the dot product and δ_{pq} are symmetric, the constraints $\mathbf{I}^{[p]} \cdot \mathbf{I}^{[q]} = \delta_{pq}$ and $\mathbf{I}^{[q]} \cdot \mathbf{I}^{[p]} = \delta_{qp}$ are the same, and the two corresponding Lagrange multipliers λ_{pq} and λ_{qp} are then equal.

When the constrained minimum is reached, the Euler-Lagrange equations corresponding to $E^*(\mathcal{B}, \lambda)$ with respect to $\mathbf{I}^{[k]}$ are: $\forall k \in [1, m]$,

$$\mathcal{L}^{[k]} + \sum_{(p,q)} \lambda_{pq} \frac{\partial \mathbf{I}^{[p]}}{\partial \mathbf{I}^{[k]}} \cdot \mathbf{I}^{[q]} + \sum_{(p,q)} \lambda_{qp} \frac{\partial \mathbf{I}^{[q]}}{\partial \mathbf{I}^{[k]}} \cdot \mathbf{I}^{[p]}$$
$$= \mathcal{L}^{[k]} + \sum_{q=1}^m \lambda_{kq} \mathbf{I}^{[q]} + \sum_{p=1}^m \lambda_{pk} \mathbf{I}^{[p]}$$
$$= \mathcal{L}^{[k]} + 2\sum_{l=1}^m \lambda_{kl} \mathbf{I}^{[l]} = 0$$

and the final set of Euler-Lagrange equations of $E^*(\mathcal{B}, \lambda)$ with respect to $\mathbf{I}^{[k]}$ and λ_{pq} writes:

$$\begin{cases} \mathcal{L}^{[k]} + 2\sum_{l=1}^m \lambda_{kl} \mathbf{I}^{[l]} = 0 & \text{(a)} \\ \mathbf{I}^{[p]} \cdot \mathbf{I}^{[q]} = \delta_{pq} \quad (k, p, q \in [1, m]) & \text{(b)} \end{cases} \quad (5)$$

Finding formally the λ_{kl} reached at the minimum is performed as follows: we take the dot product of the lth Eq. of (5a) with the vector $\mathbf{I}^{[k]}$:

$$\mathcal{L}^{[l]} \cdot \mathbf{I}^{[k]} + 2\sum_{p=1}^m \lambda_{pl} \mathbf{I}^{[p]} \cdot \mathbf{I}^{[k]} = 0$$

then simplify it using the orthonormal relations (5(b)):

$$\lambda_{kl} = -\frac{\mathcal{L}^{[l]} \cdot \mathbf{I}^{[k]}}{2}$$

Finally, replacing the λ_{kl} in (5(a)) gives the vector gradient descent that minimizes (4) while *preserving the orthonormal constraints (1)*:

$$\frac{\partial \mathbf{I}^{[k]}}{\partial t} = -\mathcal{L}^{[k]} + \sum_{l=1}^m \big(\mathcal{L}^{[l]} \cdot \mathbf{I}^{[k]}\big) \mathbf{I}^{[l]} \qquad (6)$$

where

$$\mathcal{L}_i^{[k]} = \alpha\big(I_i^{[k]} - I_{i_0}^{[k]}\big) - \operatorname{div}\left(\frac{\phi'\big(\big\|\nabla\mathbf{I}^{[k]}\big\|\big)}{\big\|\nabla\mathbf{I}^{[k]}\big\|}\nabla I_i^{[k]}\right) \quad (7)$$

The obtained Eq. (6) is a set of m coupled vector PDE's (i.e $m \times n$ scalar PDE's where the coupling between vectors *and* vector components is clearly present), which allows to regularize any field of orthonormal vector sets, preserving the orthonormal structure of the vectors during the PDE evolution.

Note.   The kth Lagrangian vector $\mathcal{L}^{[k]}$ of the unconstrained functional $E(\mathcal{B})$ can be seen as a pure *diffusion force*, acting on the vector $\mathbf{I}^{[k]}$ (a physical interpretation of this vector is provided in Section 5.2). Actually, one can note the clear separation in the PDE (6) between *the unconstrained lagrangians* $\mathcal{L}^{[k]}$ that are responsible for the regularization behavior and *the coupling term* $\sum_{l=1}^m (\mathcal{L}^{[l]} \cdot \mathbf{I}^{[k]})\mathbf{I}^{[l]}$ that allows the orthonormal constraints to be preserved.

This opens interesting possibilities: We may for instance replace the simple ϕ-function lagrangian term by more complex enhancement terms adapted to specific regularization problems, even if it doesn't come from variational principles (as for instance those proposed in Osher and Rudin (1990), Sapiro and Ringach (1996), Tschumperlé and Deriche (2001a, 2002), Weickert (1998), and Weickert and Schnörr (2001)). On can also think to use this general equation (6) to solve other orthonormal constraints related problems (image matching, edge enhancement).

From now on, we will study some particular cases of orthonormal vector sets, and the corresponding equations and applications.

4.   Direction Diffusion

Vector direction diffusion has already been studied in Bertalmio et al. (2001), Chan and Shen (2001a),

Perona (1998), Tang et al. (2000), Tschumperlé and Deriche (2001a), and Vese and Osher (2002). It consists of regularizing fields $\mathbf{I}$ of unit vectors $\mathbf{I}(x) \in S^n$. Actually, this problem can be seen as a particular case of our orthonormal vector set framework, where the vector sets $\mathcal{B}(\mathbf{x})$ are restricted to a single vector $\mathcal{B}(\mathbf{x}) = \{\mathbf{I}(\mathbf{x})\}$.

Indeed, as mentioned in Section 2, the orthonormal constraints (1) are reduced to the unitary norm constraint: $\forall \mathbf{x} \in \Omega, \|\mathbf{I}(\mathbf{x})\| = 1$.
The corresponding functional (4) also reduces to:

$$E(\mathcal{B}) = E(\mathbf{I}) = \int_\Omega (\alpha \|\mathbf{I} - \mathbf{I}_0\|^2 + \phi(\|\nabla \mathbf{I}\|)) \, d\Omega$$

and the resulting constraint-preserving PDE (6) writes in this case:

$$\frac{\partial \mathbf{I}}{\partial t} = -\mathcal{L} + (\mathcal{L} \cdot \mathbf{I}) \mathbf{I} \qquad (8)$$

where $\mathcal{L}_i = \alpha(I_i - I_{i_0}) - \text{div}(\frac{\phi'(\|\nabla \mathbf{I}\|)}{\|\nabla \mathbf{I}\|} \nabla I_i)$.

Note that the velocity in (8) is simply the projection of the vector $-\mathcal{L}$ into the space orthogonal to $\mathbf{I}$. This equation can be highly simplified: From the spatial derivations of $\|\mathbf{I}(\mathbf{x})\|^2 = 1$, we find:

$$\forall a \in [1, p], \quad \mathbf{I} \cdot \frac{\partial \mathbf{I}}{\partial x_a} = 0 \quad \text{and} \quad \Delta \mathbf{I} \cdot \mathbf{I} = -\|\nabla \mathbf{I}\|^2 \tag{9}$$

Developing the divergence in each $\mathcal{L}_i$:

$$\text{div}(A \nabla I_i) = A \Delta I_i + \nabla A \cdot \nabla I_i$$

where $A = \frac{\phi'(\|\nabla \mathbf{I}\|)}{\|\nabla \mathbf{I}\|}$. If we note by $\mathbf{d}$ the vector defined by $d_i = \text{div}(A \nabla I_i)$, with $i = 1 \ldots n$:

$$\begin{aligned}
\mathbf{d} \cdot \mathbf{I} &= A \Delta \mathbf{I} \cdot \mathbf{I} + \sum_{i=1}^n \sum_{a=1}^p \frac{\partial A}{\partial x_a} \frac{\partial I_i}{\partial x_a} I_i \\
&= A \Delta \mathbf{I} \cdot \mathbf{I} + \sum_{a=1}^p \frac{\partial A}{\partial x_a} \frac{\partial \mathbf{I}}{\partial x_a} \cdot \mathbf{I}
\end{aligned}$$

The Eq. (9) allow the simplification:

$$\mathbf{d} \cdot \mathbf{I} = -\phi'(\|\nabla \mathbf{I}\|)\|\nabla \mathbf{I}\|$$

Then, the diffusion PDE (8) becomes:

$$\begin{aligned}
\frac{\partial I_i}{\partial t} = {}& \text{div}\left(\frac{\phi'(\|\nabla \mathbf{I}\|)}{\|\nabla \mathbf{I}\|} \nabla I_i \right) + \phi'(\|\nabla \mathbf{I}\|)\|\nabla \mathbf{I}\| I_i \\
& + \alpha(I_{i_0} - (\mathbf{I}_0 \cdot \mathbf{I}) I_i)
\end{aligned} \tag{10}$$

This PDE regularizes unit vector fields, using general ϕ-functionals. Note that the PDE's proposed in Bertalmio et al. (2001), Chan and Shen (2001a), and Tang et al. (2000) are a restriction of (10) to

$$\alpha = 0 \quad \text{and} \quad \phi(s) = s^r \quad (r = 1, 2)$$

Our orthonormal vector sets framework allows to include previous works on unit vector diffusion (Bertalmio et al., 2001; Chan and Shen, 2001a; Perona, 1998; Tang et al., 2000), in a more general framework of orientation regularization.

Evolution of norm constrained vector fields has application for denoising chromaticity features in color images. Remind that a color image $\mathbf{I} = (R, G, B)^T$ can be decomposed into a chromaticity vector field $\mathbf{u} = \frac{\mathbf{I}}{\|\mathbf{I}\|}$ and a brightness (scalar) image $\|\mathbf{I}\|$. Regularizing these two attributes with two different PDE's gives better control on the color image restoration. In Section 7, we present some chromaticity denoising results using our constrained equation (10).

5. 3D Orthogonal Matrices Diffusion

We are now interested in another particular case of orthonormal vector sets: 3D orthonormal matrices. We consider then orthonormal vector bases fields ($m = n = 3$) and for simplicity reasons, we denote the three basis vectors by:

$$\mathbf{I} = \mathbf{I}^{[1]}, \quad \mathbf{J} = \mathbf{I}^{[2]} \quad \text{and} \quad \mathbf{K} = \mathbf{I}^{[3]} \quad \text{then}$$
$$\mathcal{B} = \{\mathbf{I}, \mathbf{J}, \mathbf{K}\}$$

As mentioned in Section 2, such datasets can represent fields of orthogonal matrices $\mathcal{R} \in O(3)$, since the columns of these matrices form an orthonormal vector basis $\mathcal{B}$ (Fig. 4). Note also that the sign of the determinant $\det(\mathcal{R})$ is an information that can be retrieved from the orthonormal vector basis $\mathcal{B}$, which is *direct* (then $\det(\mathcal{R}) = +1$) or *indirect* (then $\det(\mathcal{R}) = -1$).
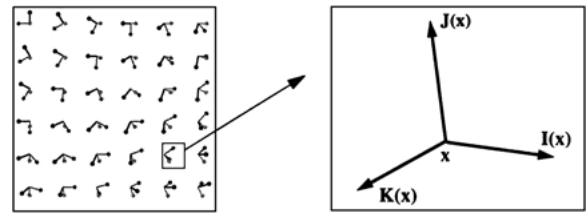

Figure 4. Field of 3D orthonormal vector bases.

5.1. Evolution Equations

In order to regularize $\mathcal{B}$ while preserving discontinuities, we minimize the functional (4), with $m = n = 3$:

$$E(\mathcal{B}) = \int_\Omega \frac{\alpha}{2}(\|\mathbf{I} - \mathbf{I}_0\|^2 + \|\mathbf{J} - \mathbf{J}_0\|^2 + \|\mathbf{K} - \mathbf{K}_0\|^2)$$
$$+ \phi(\|\nabla\mathbf{I}\|) + \phi(\|\nabla\mathbf{J}\|) + \phi(\|\nabla\mathbf{K}\|)\, d\Omega$$

Using the general solution (6), we can write the corresponding constrained set of 3D vector diffusion PDE's:

$$\begin{cases} \mathbf{I}_t = \mathcal{L}^{\mathbf{I}} - (\mathcal{L}^{\mathbf{I}} \cdot \mathbf{I})\mathbf{I} - (\mathcal{L}^{\mathbf{J}} \cdot \mathbf{I})\mathbf{J} - (\mathcal{L}^{\mathbf{K}} \cdot \mathbf{I})\mathbf{K} \\ \mathbf{J}_t = \mathcal{L}^{\mathbf{J}} - (\mathcal{L}^{\mathbf{I}} \cdot \mathbf{J})\mathbf{I} - (\mathcal{L}^{\mathbf{J}} \cdot \mathbf{J})\mathbf{J} - (\mathcal{L}^{\mathbf{K}} \cdot \mathbf{J})\mathbf{K} \\ \mathbf{K}_t = \mathcal{L}^{\mathbf{K}} - (\mathcal{L}^{\mathbf{I}} \cdot \mathbf{K})\mathbf{I} - (\mathcal{L}^{\mathbf{J}} \cdot \mathbf{K})\mathbf{J} - (\mathcal{L}^{\mathbf{K}} \cdot \mathbf{K})\mathbf{K} \end{cases}$$
$$(11)$$

where $\mathcal{L}^{\mathbf{I}}$, $\mathcal{L}^{\mathbf{J}}$, $\mathcal{L}^{\mathbf{K}}$ are the unconstrained functional Lagrangian vectors, associated to the vectors $\mathbf{I}$, $\mathbf{J}$, $\mathbf{K}$ and defined by (7). Note that this equation can be equivalently written with a *matrix PDE flow*:

$$\frac{\partial \mathcal{R}}{\partial t} = \mathbf{L} - \mathcal{R}\mathbf{L}^{\mathbf{T}}\mathcal{R} \qquad (12)$$

where the matrices $\mathcal{R}$ and $\mathbf{L}$ are defined column by column:

$$\mathcal{R} = (\mathbf{I} \,|\, \mathbf{J} \,|\, \mathbf{K}) \quad \text{and} \quad \mathbf{L} = (\mathcal{L}^{\mathbf{I}}|\mathcal{L}^{\mathbf{J}}|\mathcal{L}^{\mathbf{K}})$$

The Eq. (12) corresponds then to an *orthogonal matrix-preserving regularizing PDE*. Note that its extension to higher matrix dimensions O(n) is also valid. Developing (12) with

$$\mathcal{R} = \left(\mathbf{I}^{[1]} \big| \cdots \big| \mathbf{I}^{[n]}\right) \quad \text{and} \quad \mathbf{L} = \left(\mathcal{L}^{[1]} \big| \cdots \big| \mathcal{L}^{[n]}\right)$$

gives the expression of the general orthonormal vector sets evolution (6) for $m = n$. (see also (Chefd'hotel et al., 2002) for interesting developments on other matrix-valued flows).

5.2. A Physical Interpretation

$\mathcal{B}(\mathbf{x}) = \{\mathbf{I}(\mathbf{x}), \mathbf{J}(\mathbf{x}), \mathbf{K}(\mathbf{x})\}$ can be seen as a solid object composed of three orthogonal rigid stems of unit length, fixed at the same point $\mathbf{x}$, and submitted to forces $\mathbf{f}^{\mathbf{I}}$, $\mathbf{f}^{\mathbf{J}}$ and $\mathbf{f}^{\mathbf{K}}$ respectively (Fig. 5).

A rotation around $\mathbf{x}$ is obviously the only motion that can perform $\mathcal{B}$. Actually, each force $\mathbf{f}^{\mathbf{I}}$, $\mathbf{f}^{\mathbf{J}}$ and $\mathbf{f}^{\mathbf{K}}$
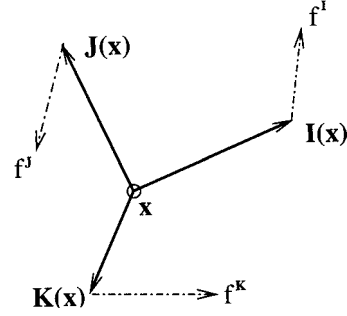

Figure 5.   A solid object $\mathcal{B}$, submitted to forces.

induces a mechanic momentum on this object:

$$\omega_{\mathbf{I}} = \mathbf{I} \times \mathbf{f}^{\mathbf{I}}, \quad \omega_{\mathbf{J}} = \mathbf{J} \times \mathbf{f}^{\mathbf{J}}, \text{ and } \quad \omega_{\mathbf{K}} = \mathbf{K} \times \mathbf{f}^{\mathbf{K}}$$

Where $\times$ designates the usual cross product in $\mathbb{R}^3$. Then, the total momentum applied to the object $\mathcal{B}$ is given by:

$$\omega = \omega_{\mathbf{I}} + \omega_{\mathbf{J}} + \omega_{\mathbf{K}}$$

i.e

$$\omega = (\mathbf{I} \times \mathbf{f}^{\mathbf{I}}) + (\mathbf{J} \times \mathbf{f}^{\mathbf{J}}) + (\mathbf{K} \times \mathbf{f}^{\mathbf{K}}) \qquad (13)$$

If we suppose that $\mathcal{B}$ has an unit moment of inertia, we can express the velocities $\mathbf{v}^{\mathbf{I}}$, $\mathbf{v}^{\mathbf{J}}$ and $\mathbf{v}^{\mathbf{K}}$ at each free extremity of the stems, corresponding to *the constrained motion* of the solid:

$$\begin{cases} \mathbf{v}^{\mathbf{I}} = \omega \times \mathbf{I} \\ \mathbf{v}^{\mathbf{J}} = \omega \times \mathbf{J} \\ \mathbf{v}^{\mathbf{K}} = \omega \times \mathbf{K} \end{cases}$$

Developing these expressions, using the double vector product formula $\mathbf{u} \times (\mathbf{v} \times \mathbf{w}) = (\mathbf{u}.\mathbf{w})\mathbf{v} - (\mathbf{u}.\mathbf{v})\mathbf{w}$ and the orthogonal properties $\mathbf{I}^{[k]} \cdot \mathbf{I}^{[l]} = \delta_{kl}$, leads to:

$$\begin{cases} \mathbf{v}^{\mathbf{I}} = \mathbf{f}^{\mathbf{I}} - (\mathbf{f}^{\mathbf{I}}.\mathbf{I})\mathbf{I} - (\mathbf{f}^{\mathbf{J}}.\mathbf{I})\mathbf{J} - (\mathbf{f}^{\mathbf{K}}.\mathbf{I})\mathbf{K} \\ \mathbf{v}^{\mathbf{J}} = \mathbf{f}^{\mathbf{J}} - (\mathbf{f}^{\mathbf{I}}.\mathbf{J})\mathbf{I} - (\mathbf{f}^{\mathbf{J}}.\mathbf{J})\mathbf{J} - (\mathbf{f}^{\mathbf{K}}.\mathbf{J})\mathbf{K} \\ \mathbf{v}^{\mathbf{K}} = \mathbf{f}^{\mathbf{K}} - (\mathbf{f}^{\mathbf{I}}.\mathbf{K})\mathbf{I} - (\mathbf{f}^{\mathbf{J}}.\mathbf{K})\mathbf{J} - (\mathbf{f}^{\mathbf{K}}.\mathbf{K})\mathbf{K} \end{cases}$$

A velocity is an infinitesimal variation of a vector during the time ∂t:

$$\frac{\partial \mathbf{I}}{\partial t} = \mathbf{v}^{\mathbf{I}}, \quad \frac{\partial \mathbf{J}}{\partial t} = \mathbf{v}^{\mathbf{J}}, \quad \frac{\partial \mathbf{K}}{\partial t} = \mathbf{v}^{\mathbf{K}}$$

If we choose the forces $\mathbf{f^I}, \mathbf{f^J}, \mathbf{f^K}$ to be defined by (7), we find the expected regularization PDE (12) that preserves the orthogonal constraints: the functional (4) can then be seen as a mechanic energy associated to a rigid object $\mathcal{B}$, submitted to three *pure diffusion forces* $\mathbf{f^I}, \mathbf{f^J}, \mathbf{f^K}$. The obtained PDE's are the expression of the *instant rotations* applied to $\mathcal{B}$ in order to minimize this energy.

5.3.   3D Implementation Issue

The PDE flows (6), (10), (12) acting on orthonormal vector sets have this particular form:

$$\frac{\partial \mathbf{I}^{[k]}}{\partial t} = \beta^{[k]} \quad \text{with} \begin{cases} \beta^{[k]} \perp \mathbf{I}^{[k]} \\ \|\mathbf{I}^{[k]}\| = 1 \end{cases}$$

Indeed, if we use the general expression (6) of orthonormal vector sets evolution for $\beta^{[k]}$:

$$\begin{aligned} \beta^{[k]}.\mathbf{I}^{[k]} &= \left(-\mathcal{L}^{[k]} + \sum_{l=1}^{m} (\mathcal{L}^{[l]}.\mathbf{I}^{[k]})\mathbf{I}^{[l]} \right).\mathbf{I}^{[k]} \\ &= -\mathcal{L}^{[k]}.\mathbf{I}^{[k]} + \mathcal{L}^{[k]}.\mathbf{I}^{[k]} \\ &= 0 \end{aligned}$$

The PDE velocity $\beta^{[k]}$ is then anytime orthogonal to the corresponding vector $\mathbf{I}^{[k]}$ (It is generally the case for vector PDE's acting on *orientation features*, as in Chan and Shen (2001a), Kimmel and Sochen (2002), Perona (1998), Tang et al. (2000), Tschumperlé and Deriche (2001a) and Vese and Osher (2002).

This means that the vector $\mathbf{I}^{[k]}(\mathbf{x})$ should theoretically perform a rotation motion around $\mathbf{x}$, preserving its norm. But using *classic explicit schemes* as

$$\mathbf{I}^{[k]}_{(t+dt)} = \mathbf{I}^{[k]}_{(t)} + dt\,\beta^{[k]} \quad \text{where} \quad 0 < dt \ll 1$$

leads to numerical errors since the underlying manifold is non-flat and the unit norms of the vectors $\mathbf{I}^{[k]}$ are not preserved (Fig. 6).

In Bertalmio et al. (2001) and Tang et al. (2000) for direction vector diffusion purposes, this problem is avoided thanks to a re-normalization step of the vector $\mathbf{I}^{[k]}$ after few PDE iterations (see also recent developments in Vese and Osher (2002) for an interesting alternative solution). Anyway, this method cannot be applied when dealing with orthonormal vector sets, because the orthogonal angles between vectors may not be preserved by this way.
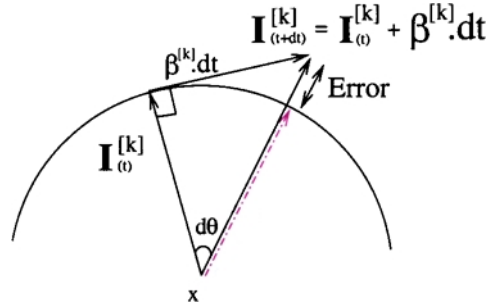

Figure 6.   Numerical errors with classic explicit schemes.

The mechanical interpretation of the 3D case (Section 5.2) provides us a simple and accurate solution to this re-normalization problem: we apply at each time step the *instant rotation* corresponding to the evolution equation (12) on the orthonormal 3D basis $\mathcal{B}$. This rotation is the same for all the vectors $\mathbf{I}, \mathbf{J}, \mathbf{K}$ (Section 5.2) and is given by the rotation vector ω, defined by the mechanic momentum:

$$\omega = (\mathbf{I} \times \mathcal{L}^{I}) + (\mathbf{J} \times \mathcal{L}^{J}) + (\mathbf{K} \times \mathcal{L}^{K})$$

where the $\mathcal{L}$ are defined by (7) and are discretized with classic finite-difference schemes (Kornprobst et al., 1998) (their discretizations will be independent of the constraints preservation). The *infinitesimal rotation* matrix Γ corresponding to the instant rotation ω is computed thanks to the Rodrigues' formula [23]:

$$\begin{aligned} \Gamma = e^{Hdt} = \mathbb{I} &+ \frac{\sin\|\omega dt\|}{\|\omega dt\|} Hdt \\ &+ \frac{1 - \cos\|\omega dt\|}{\|\omega dt\|^2} H^2 dt^2 \end{aligned}$$

where $dt > 0$ is the time step and H is the skew-symmetric matrix representing the cross-product with the rotation vector ω:

$$H = \begin{pmatrix} 0 & -\omega_z & \omega_y \\ \omega_z & 0 & -\omega_x \\ -\omega_y & \omega_x & 0 \end{pmatrix}$$

The evolution scheme for the matrix-valued PDE (12) in the 3D case is then simply:

$$\mathcal{R}_{(t+dt)} = \Gamma \mathcal{R}_{(t)}$$

where

$$\mathcal{R} = (\mathbf{I} \mid \mathbf{J} \mid \mathbf{K})$$

It provides a numerical way to preserve the unitary norm, as well as the orthogonal angles (the column vectors $\mathbf{I}$, $\mathbf{J}$, $\mathbf{K}$ of $\mathcal{R}$ perform *the same infinitesimal rotation* Γ at each time step t). The numerical error, due to ($dt \neq 0$), is only present in the rotation angle $\|\boldsymbol{\omega}\|$, but doesn't affect the orthonormal vector bases configuration. Note also that this scheme naturally *preserves the determinants* of the corresponding orthogonal matrices $\mathcal{R}$, during the flow. Indeed,

$$\begin{aligned}
\det\big(\mathcal{R}_{(t+dt)}\big) &= \det\big(\Gamma \mathcal{R}_{(t)}\big) \\
&= \det(\Gamma)\det\big(\mathcal{R}_{(t)}\big) \qquad (14) \\
&= \det\big(\mathcal{R}_{(t)}\big)
\end{aligned}$$

since by construction $\Gamma \in SO(3)$ and then $\det(\Gamma) = +1$. More particularly, it means that a rotation $\mathcal{R} \in SO(3)$ *cannot be transformed to a rotoinversion* during the orthogonal PDE flow (12). Note that extensions of these schemes for $m = n > 3$ has been recently proposed in Chefd'hotel et al. (2002), generalizing the use of exponential maps to build general matrix PDE flows on constrained manifolds.

6. Applications of Orthogonal Matrix Flows

In this section, we present two different applicative problems that can be naturally solved using our orthogonal-matrix preserving flow (12).

6.1. Estimated Camera Motion Regularization

Suppose one wants to regularize a video camera motion. Taking a real movie sequence as an input, a first process estimates the camera motion, then outputs two temporal sequences, one corresponding to the camera translation (change of the view point) and the second to the camera rotation (change of the view angle) (see Faugeras (1993) and RealviZ (1999) for algorithms and products that perform this estimation).

These two outputs may be noisy (motion estimation algorithms often use correspondence points computed from the movie images which are very sensitive to the noise) and a motion regularization process may be needed (Fig. 7). This is the case for instance, when
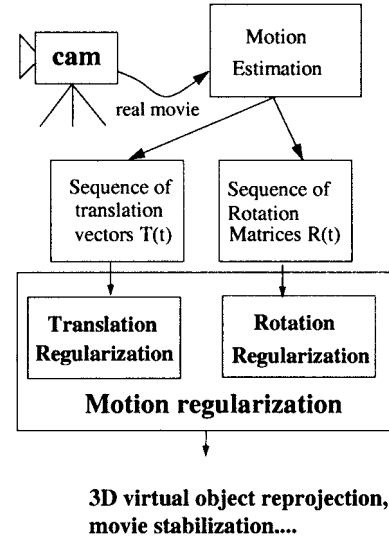

Figure 7. Camera motion regularization.

one wants to re-project with a smoother way 3D virtual objects on a real movie, using the estimated motion information (this new technique attracts a growing interest in the domain of special effects).

The translation part $\mathbf{T} = (T_x, T_y, T_z)^{\mathrm{T}}$ of this camera motion can be easily restored, using classic unconstrained vector-valued PDE's (Blomgren and Chan, 1998; Kimmel et al., 2000; Sapiro and Ringach, 1996; Sochen et al., 1997; Sternberg, 1991; Tschumperlé and Deriche, 2001a; Weickert, 1998). Regularizing the sequence of the camera orientations may be more complicated.

When dealing with rotation matrices, a natural idea is to decompose these matrices into more simple data that are easy to regularize (usually Euler angles, unit quaternions or rotation vectors), then reconstruct the final rotation field from smoothed versions of these data (Fig. 8).

However this method has some drawbacks: First, the conversions often induce numerical imprecisions.
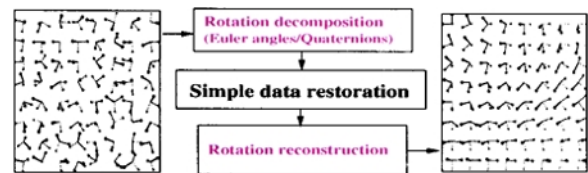

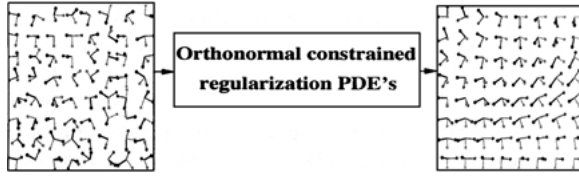Figure 8. Decomposition of the rotations for orientation regularization purposes.

Figure 9. Direct rotation field restoration using orthonormal vector sets.

Second, the rotation decomposition *is not unique*. It would introduce annoying discontinuities in the decomposed data, even if the initial rotation field is perfectly smooth. These discontinuities are coming from:

- The 2π-periodicity ambiguity of the Euler angles or the norms of the rotation vectors.
- The double representation of a single rotation by two equivalent quaternions q and $-q$.

It has a large influence on the anisotropic regularization behavior by detecting non-existent discontinuities which perturb the diffusion process.

Actually, using the orthogonal-preserving flow (12) coming from the framework of orthonormal vector sets, solves this problem: we apply directly the PDE (12) on the rotation matrices sequence in order to regularize it. No rotation decompositions are needed anymore, and there are no false discontinuities problems since we work directly on the matrix coefficients which form a unique representation of $\mathcal{R}$ (Fig. 9).

Note that this approach is valid, since the matrix determinant $\det(\mathcal{R}) = +1$ is preserved along the regularization flow, thanks to the determinant property (14). One result obtained on a real camera estimation sequence is presented in Section 7.

6.2. Regularization of DT-MRI Volumes

Let us denote by P(3) the space of symmetric and positive-definite matrices. We are now interested in regularizing fields

$$\mathcal{T} : \Omega \to P(3)$$

of diffusion tensors coming from DT-MRI imaging.

This recent and non-invasive 3D medical image modality consists in measuring the water molecule motion in the white matter tissues, using magnetic resonance techniques. Each voxel $\mathcal{T}(\mathbf{x})$ of the acquired image $\mathcal{T}$ is a symmetric and positive definite 3×3 matrix

that defines the local fiber structure of the tissues, as described in Granlund and Knutsson (1995), Le Bihan (2000), Poupon (1999) and Vemuri et al. (2001).

Regularizing such fields is an interesting process:

- It constructs smoothed versions of the tissues fibers, allowing to retrieve interesting 'scale-space' properties of these physiological structures.
- It denoises the datasets and more coherent physiological indices (as *VR*, *RA*, *FA*, ... see Le Bihan (2000) and Poupon (1999)) can be computed from the regularized tensors.

Actually, the fiber orientations are not explicitly given by the matrices $\mathcal{T}(\mathbf{x})$, but can be retrieved by a *spectral decomposition*

$$\forall \mathbf{x} \in \Omega, \quad \mathcal{T}(\mathbf{x}) = \mathcal{R}(\mathbf{x})\mathbf{D}(\mathbf{x})\mathcal{R}(\mathbf{x})^{\mathbf{T}}$$

where $\mathcal{R}(\mathbf{x}) = (\mathbf{I}(\mathbf{x})|\mathbf{J}(\mathbf{x})|\mathbf{K}(\mathbf{x}))$ and

$$\mathbf{D}(\mathbf{x}) = \begin{pmatrix} \lambda_1(\mathbf{x}) & 0 & 0 \\ 0 & \lambda_2(\mathbf{x}) & 0 \\ 0 & 0 & \lambda_3(\mathbf{x}) \end{pmatrix}$$

$\mathcal{R}$ is a field of 3×3 *orthogonal matrices* that represent *the tensors orientations* and whose columns $\mathbf{I}$, $\mathbf{J}$ and $\mathbf{K}$ are the unit eigenvectors $\mathcal{T}$, while $\mathbf{D}$ is the field of the *tensors diffusivities* which are positive values ($\mathcal{T}$ is positive-definite). A natural 3D representation of $\mathcal{T}$ is then a field of ellipsoids whose axes and radiuses are respectively given by the eigenvectors of $\mathcal{T}$ and the columns of $\mathcal{R}$ (Fig. 10).

Retrieving the fiber bundles is then made by following the main direction $\mathbf{I}$ of the tensors at each voxel of the volume $\mathcal{T}$.

Interesting works on DT-MRI regularization can be found in Chefd'hotel et al. (2002), Coulon et al. (2001a, 2001b), Poupon et al. (1998), Tschumperlé and Deriche
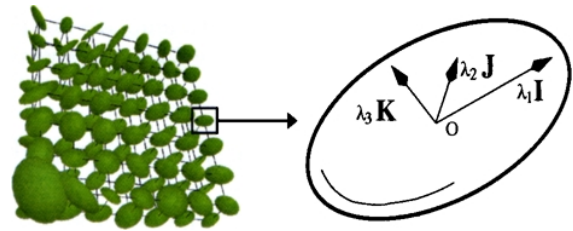

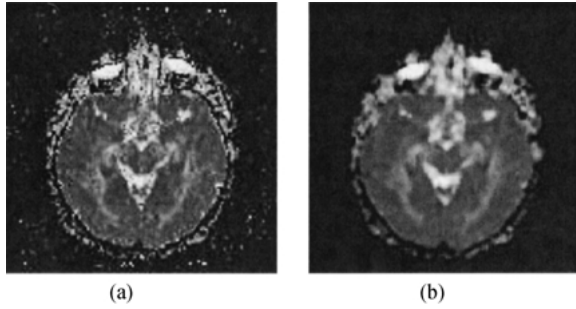*Figure 10.* 3D diffusion tensor field $\mathcal{T} : \Omega \to P(3)$.

Figure 11. Regularization of DT-MRI diffusivities **D**. (a) Mean diffusivity $(\lambda_1 + \lambda_2 + \lambda_3)/3$ of a brain DT-MRI. (b) Regularized diffusivities with (3) and $\phi(s) = s$.

(2001b) and Vemuri et al. (2001). Instead of regularizing directly the matrix field $\mathcal{T}$ with positive-definite preserving flows, we propose to act both on the tensor orientations $\mathcal{R}$ and diffusivities **D** by applying two different PDE's (this separate regularization is justified in Chefd'hotel et al. (2002) and Tschumperlé and Deriche (2001b).

Concerning the tensor diffusivity part, the field **D** can be regularized with classical vector-valued regularization methods that must anyway satisfy the maximum principle [4], in order to ensure the definite-positiveness of the tensors. Suitable PDE's can be found for instance in Blomgren and Chan (1998), Kimmel et al. (2000), Sapiro and Ringach (1996), Sochen et al. (1997), Sternberg (1991), Tschumperlé and Deriche (2001a) and Weickert (1998) (Fig. 11).

As for the tensor orientation field $\mathcal{R}$, it can be easily regularized with our orthogonal-preserving flow (12). Anyway, we have to take care of the non-uniqueness of the spectral decomposition: flipping one eigenvector direction while keeping its orientation gives the same tensor $\mathcal{T}$. To overcome this problem, a local eigenvector alignment process is made before applying the PDE on each tensor of the field $\mathcal{T}$, and for each time-step t. The idea is to align the neighboring eigenvector directions with the current one. This is done by minimizing the angles between them, constraining the dot product to be positive by flipping the neighboring eigenvectors if necessary:

$$\forall \mathbf{y} \in \mathcal{V}(\mathbf{x}), \ \mathbf{I}^{[\tilde{k}]}(\mathbf{y}) = \text{sign}\big(\mathbf{I}^{[k]}(\mathbf{y}) \cdot \mathbf{I}^{[k]}(\mathbf{x})\big)\mathbf{I}^{[k]}(\mathbf{y})$$

where $\mathcal{V}(\mathbf{x})$ is a neighborhood of $\mathbf{x}$ (see also Coulon et al. (2001a, 2001b) and Tschumperlé and Deriche (2001a) for similar eigenvector flipping methods).

This local operation ensures we work only on the tensor orientations, without taking into account the eigen-

vector directions that are dependent of the spectral decomposition algorithm.

Application results of this regularization method on real DT-MRI datasets is illustrated in Section 7, with the reconstruction of fibers map in the white matter of the brain.

7. Experimental Results

We applied the orthonormal vector sets preserving equations (6), (10), (12) proposed in this paper, on synthetic and real datasets, using the numerical scheme proposed in Section (5.3) (this is possible since the dimensions of the examples are less or equal than 3). The results are displayed column by column on Figs. 12 and 13:

- *Direction vector regularization*: The application of (10) on a field of 2D direction vectors allows to smooth the noisy field, without losing the important global structures (discontinuities and singular points) thanks to the anisotropic behavior of the ϕ-function diffusion (Fig. 12(1))
- *Noisy chromaticity color image restoration*: This is an application of (10) for the 3D case, with vectors $\mathbf{I} = (R, G, B)^{\mathrm{T}}$. Denoising the direction of color vectors allows to act only on the chromaticity part of these colors. If we assume that the noise if purely chromatic, we get much better results than classic unconstrained color regularization PDE's (Fig. 12(2)).
- *Orthogonal matrix diffusion*: Figure 12(3) illustrates how we can deal with anisotropic behavior for orthogonal matrix diffusion with (12). We used here a total variation functional $\phi(s) = s$, in order to restore a synthetic field of 3×3 rotation matrices involving a triple junction.
- *Camera motion regularization*: We display on Fig. 13(4), images of a video sequence where a virtual 3D teapot has been inserted. Estimating the camera motion of the original movie (Fig. 13(4a)) gives a sequence of rotations and translations. The restoration of these sequences, using (12) and (3) allows to project in a smooth way, the 3D teapot, leading to a more realistic sequence (here the original motion is known to be smooth) (Fig. 13(4c)). Figure 13(5a) shows that the restoration of the orientation part of the motion has also a regularizing effect on the corresponding Euler angles. *Note that we didn't regularize the Euler-angles themselves*, but acted only on the coefficients of the original rotation
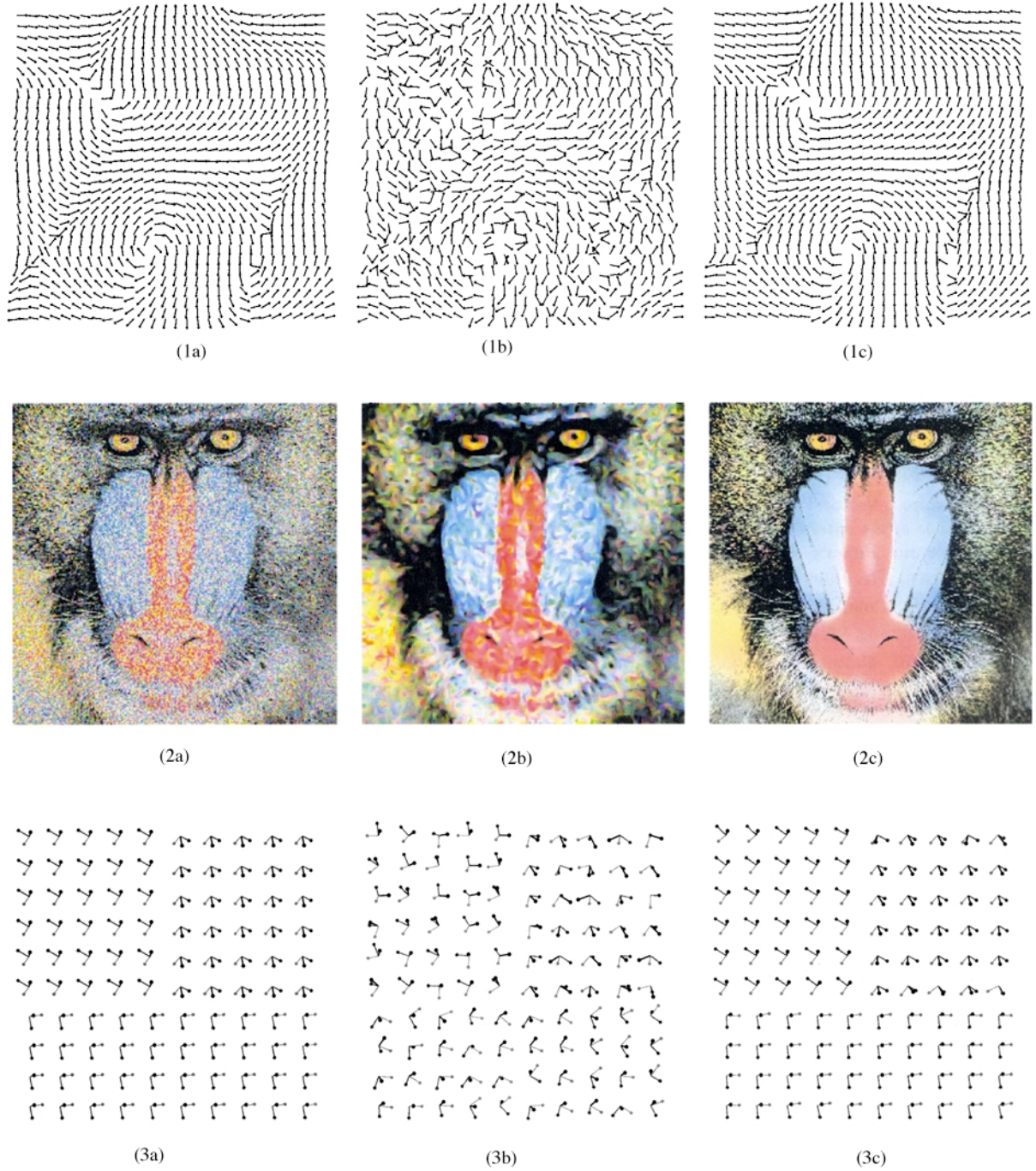
(1a)   (1b)   (1c)

(2a)   (2b)   (2c)

(3a)   (3b)   (3c)

Figure 12.   Application of orthonormal vector sets regularization framework for restoration of unit vector fields (1), color chromaticity (2) and 3D rotations fields (3). (1a) Synthetic 2D field of 2D direction vectors. (1b) With orientation noise added to (1a). (1c) Restored field (Eq. (10), with $\phi(s) = \sqrt{1 + s^2}$). (2a) Noisy chromaticity color image. (2b) Regularization with unconstrained color ϕ-functional (Eq. (3), with $\phi(s) = \sqrt{1 + s^2}$). (2c) Chromaticity-based restoration (Eq. (10), with $\phi(s) = s$). (3a) Synthetic 2D field of 3D rotations (with a triple junction). (3b) With orientation noise added to (4a). (3c) Restored 3D rotations field (Eq. (12), with $\phi(s) = s$).

(4a)   (4b)   (4c)

(5a)   (5b)   (5c)

(6a)   (6b)   (6c)
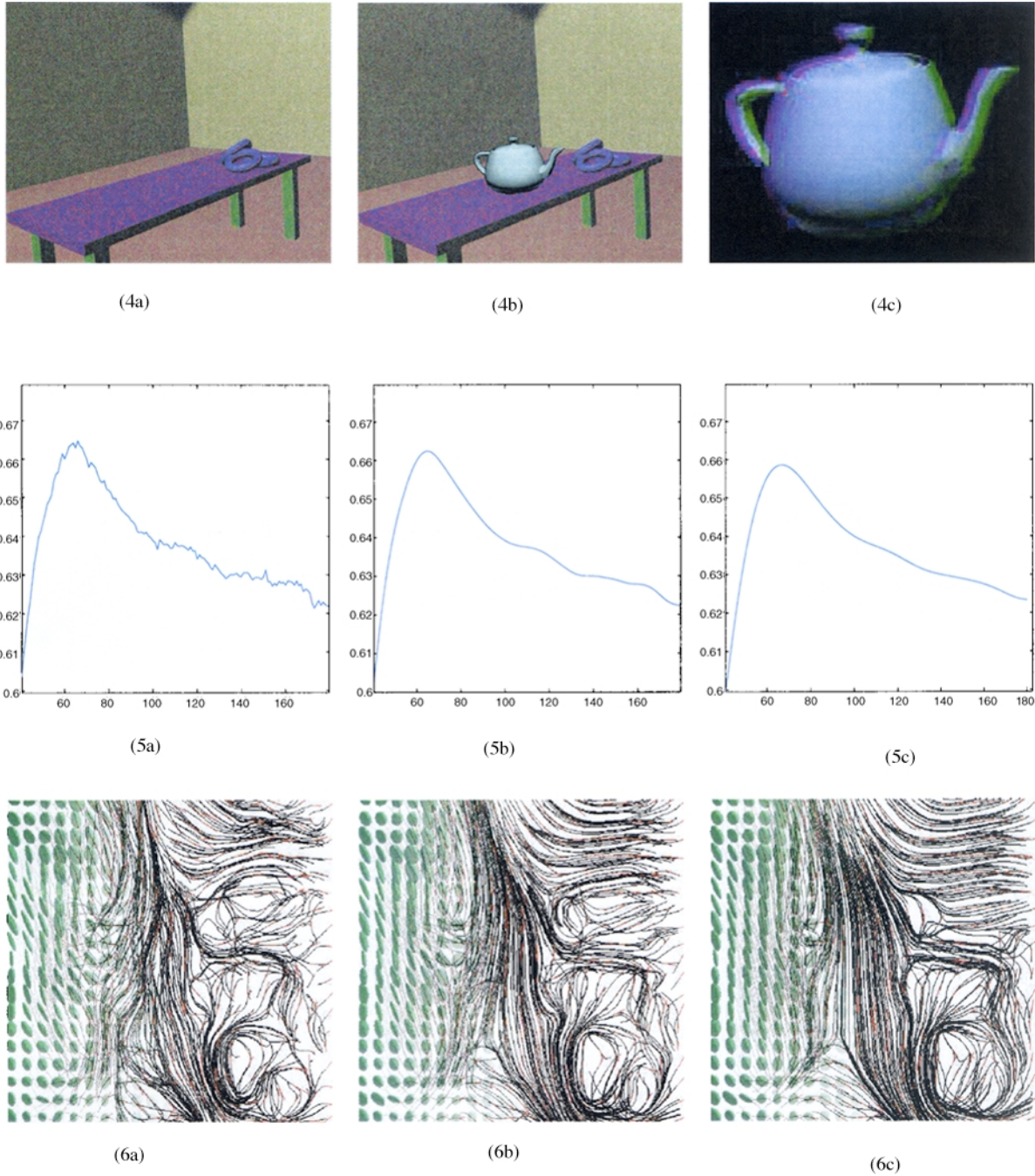
Figure 13.   Application of orthonormal vector sets regularization: Smooth reprojection of a virtual object in a real movie (4), (5) and DT-MRI images regularization and smooth fibers reconstruction (6). (4a) Synthetic movie of a 3D desk. (4b) Incrustation of a virtual 3D teapot on the desk. (4c) Difference between regularized motion and initial estimated motion from the movie. (5a) Euler angle X of the estimation of a real camera motion. (5b) Euler angle X of the regularized motion (intermediate iteration), with Eq. (12). (5c) Euler angle X of the regularized motion (at convergence), with Eq. (12). (6a) Detail of a real DT-MRI of the brain (tensors are displayed on the left, main streamlines on the right). (6b) Regularized volume, with orthogonal PDE (12) and $\phi(s) = \sqrt{1 + s^2}$ at intermediate iteration. (6c) Regularized volume, with orthogonal PDE (12) and $\phi(s) = \sqrt{1 + s^2}$ at steady state.

matrix sequence. The ϕ-function $\phi(s) = s^2$ used here has an isotropic effect. This choice is justified since the handled sequence is uni-dimensional and shouldn't contains discontinuities (the motion estimation is always done on continuous sequence of the movie).

- *Diffusion tensor restoration*: Figure 13(6) shows the application described in Section 6.2, for constructing smooth tissues fiber map in the white matter of the brain. We regularize a real DT-MRI dataset (courtesy of CEA-SHFJ (2000)) and follow at each voxel of the volume the main tensor directions which are representative of the fibers structures. Two regularization steps are shown (Fig. 13(6b) and Fig. 13(6c)). For each subfigure, the tensor field is represented with ellipsoids on the left part of the image, and with the computed streamlines on the right. Note how the computed fibers are smoothed along the PDE flow (12). Here, the gradient functional may depend on physiological attributes, as for instance functions proposed in Coulon et al. (2001a, 2001b), although we used here a classical ϕ-functional $\phi(s) = \sqrt{1 + s^2}$ Charbonnier et al. (1994).

8. Concluding Remarks

In this paper, we introduced an interesting constrained multi-valued feature: the orthonormal vector set, that is a natural generalization of the unit sphere S^n for multi-dimensions, and is well adapted to represent orientation characteristics of various datasets. We proposed a ϕ-functional based framework that allows to regularize fields of orthonormal vector sets, and used it to address a wide variety of regularization problems. First, we made the link with previous works on unit vector fields regularization with application to chromaticity denoising in color images. Second, we tackled the problems of diffusion tensor field restoration and camera motion regularization, that can find applications in medical imaging and post-production. The clear separation between the constraints and the minimizing unconstrained gradient opens new perspectives for other computer-vision problems, such as image matching or segmentation. This is on-going research.

Acknowledgments

References

Acton, S.T. 1998. Multigrid anisotropic diffusion. *IEEE Transactions on Image Processing*, 7:280–291.

Alvarez, L., Deriche, R., Weickert, J., and Sànchez, J. 2002. Dense disparity map estimation respecting image discontinuities: A PDE and scale-space based approach. *International Journal of Visual Communication and Image Representation*, Special Issue on PDE in Image Processing, Computer Vision and Computer Graphics, 13(1/2):3–21.

Alvarez, L., Lions, P.L., and Morel, J.M. 1992. Image selective smoothing and edge detection by nonlinear diffusion (II). *SIAM Journal of Numerical Analysis*, 29:845–866.

Bertalmio, M., Sapiro, G., Caselles, V., and Ballester, C. 2000. Image inpainting. In *Proceedings of the SIGGRAPH*, Kurt Akeley (Ed.), ACM Press, pp. 417–424.

Bertalmio, M., Sapiro, G., Cheng, L.T., and Osher, S. 2001. Variational problems and PDE's on implicit surfaces. In *IEEE Workshop on Variational and Level Set Methods*, Vancouver, Canada, pp. 186–193.

Blomgren, P. and Chan, T.F. 1998. Color TV: Total variation methods for restoration of vector-valued images. *IEEE Trans. Imag. Proc.*, 7(3):304–309. Special issue on PDE and Geometry-Driven Diffusion in Image Processing and Analysis.

Caselles, V., Morel, J.M., Sapiro, G., and Tannenbaum, A. 1998. Introduction to the special issue on PDE and geometry-driven diffusion in image processing and analysis. *IEEE Transactions on Image Processing*, 7(3):269–273.

Chambolle, A. and Lions, P.L. 1997. Image recovery via total variation minimization and related problems. *Nümerische Mathematik*, 76(2):167–188.

Chan, T., Kang, S.H., and Shen, J. 2000. Total variation denoising and enhancement color images based on the CB and HSV color models. *Journal of Visual Communication and Image Representation*, 12(4).

Chan, T., Sandberg, B.Y., and Vese, L. 2000. Active contours without edges for vector-valued images. *Journal of Visual Communication and Image Representation*, 11:130–141.

Chan, T. and Shen, J. 2000. Non-texture inpaintings by curvature-driven diffusions. *Journal of Visual Communication and Image Representation*, 12(4):436–449.

Chan, T. and Shen, J. 2001a. Variational restoration of nonflat image features: Models and algorithms. *SIAM Journal on Applied Mathematics*, 61(4):1338–1361.

Chan, T. and Shen, J. 2001b. Mathematical models for local nontexture inpaintings *SIAM Journal on Applied Mathematics*, 62(3):1019–1043.

Charbonnier, P., Aubert, G., Blanc-Féraud, M., and Barlaud, M. 1994. Two deterministic half-quadratic regularization algorithms for computed imaging. In *Proceedings of the International Conference on Image Processing*, 2:168–172.

Chefd'hotel, C., Tschumperlé, D., Deriche, R., and Faugeras, O. 2002. Constrained flows on matrix-valued functions: Application to diffusion tensor regularization. In *Proceedings of ECCV'02*.

Cohen, L. 1995. Auxiliary variables and two-step iterative algorithms in computer vision problems. *International Conference on Computer Vision*.

Cottet, G.H. and Germain, L. 1993. Image processing through reaction combined with nonlinear diffusion. *Mathematics of Computation*, 61(204):659–673.

Coulon, O., Alexander, D.C., and Arridge, S.R. 2001a. A geometrical approach to 3D diffusion tensor magnetic resonance image regularisation. Department of Computer Science, University College London. Technical Report.

Coulon, O., Alexander, D.C., and Arridge, S.R. 2001b. A regularization scheme for diffusion tensor magnetic resonance images. In *XVIIth International Conferenceon Information Processing in Medical Imaging*.

Dibos, F. and Koepfler, G. 1998. Global total variation minimization. CEREMADE (URACNRS 749), Technical Report 9801.

Faugeras, O. 1993. *Three-Dimensional Computer Vision: A Geometric Viewpoint*. MIT Press: Cambridge, MA.

Geman, S. and McClure, D.E. 1985. Bayesian image analysis: An application to single photon emission tomography. *Amer. Statist. Assoc.*, pp. 12–18.

Granlund, G.H. and Knutsson, H. 1995. *Signal Processing for Computer Vision*. Kluwer Academic Publishers.

Kimmel, R., Malladi, R., and Sochen, N. 2000. Images as embedded maps and minimal surfaces: Movies, color, texture, and volumetric medical images. *International Journal of Computer Vision*, 39(2):111–129.

Kimmel, R. and Sochen, N. 2002. Orientation diffusion or how to comb a porcupine. *Journal of Visual Communication and Image Representation*, Special Issue on PDE in Image Processing, Computer Vision and Computer Graphics, 13(1/2):238–248.

Kornprobst, P., Deriche, R., and Aubert, G. 1997a. Image coupling, restoration and enhancement via PDE's. In *Proceedings of the International Conference on Image Processing*, Santa Barbara, California, vol. 4, pp. 458–461.

Kornprobst, P., Deriche, R., and Aubert, G. 1997b. Nonlinear operators in image restoration. In *Proceedings of the International Conference on Computer Vision and Pattern Recognition*, Puerto Rico, IEEE Computer Society, pp. 325–331.

Kornprobst, P., Deriche, R., and Aubert, G. 1998. EDP, débruitage et réhaussement en traitement d'image: Analyse et contributions. In *11ème Congrés RFIA*, AFCET, vol. 1, pp. 277–286.

Koschan, A. 1995. A comparative study on color edge detection. In *Proceedings of the 2nd Asian Conference on Computer Vision*, Singapore, vol. 3, pp. 574–578.

Le Bihan, D. 2000. Methods and applications of diffusion mri. In *Magnetic Resonance Imaging and Spectroscopy in Medicine and Biology*, I.R. Young (Ed.). John Wiley and Sons.

Malladi, R. and Sethian, J.A. 1996. Image processing: Flows under min/max curvature and mean curvature. *Graphical Models and Image Processing*, 58(2):127–141.

Morel, J.M. and Solimini, S. 1988. Segmentation of images by variational methods: A constructive approach. *Rev. Math. Univ. Complut. Madrid*, 1:169–182.

Mumford, D. and Shah, J. 1989. Optimal approximations by piecewise smooth functions and associated variational problems. *Communications on Pure and Applied Mathematics*, 42:577–684.

Nagel, H.H. and Enkelmann, W. 1986. An investigation of smoothness constraint for the estimation of displacement vector fiels from images sequences. *IEEE Transactions on Pattern Analysis and Machine Intelligence*, 8:565–593.

Nikolova, M. and Ng, M. 2001. Fast image reconstruction algorithms combining half-quadratic regularization and preconditioning. In *Proceedings of the International Conference on Image Processing*. IEEE Signal Processing Society.

Nordström, N. 1990. Biased anisotropic diffusion—A unified regularization and diffusion approach to edge detection. *Image and Vision Computing*, 8(11):318–327.

Osher, S. and Rudin, L.I. 1990. Feature-oriented image enhancement using shock filters. *SIAM Journal of Numerical Analysis*, 27(4):919–940.

Paragios, N. and Deriche, R. 2002. Geodesic active regions: A new paradigm to deal with frame partition problems in computer vision. *International Journal of Visual Communication and Image Representation*, Special Issue on PDE in Image Processing, *Computer Vision and Computer Graphics*, 13(1/2):249–268.

Perona, P. 1998. Orientation diffusions. *IEEE Transactions on Image Processing*, 7(3):457–467.

Perona, P. and Malik, J. 1990. Scale-space and edge detection using anisotropic diffusion. *IEEE Transactions on Pattern Analysis and Machine Intelligence*, 12(7):629–639.

Poupon, C. 1999. *Détection des faisceaux de fibres de la substance blanche pour l'étude de la connectivité anatomique cérébrale*. Ph.D. thesis, Ecole Nationale Supérieure des Télécommunications.

Poupon, C., Mangin, J.F., Frouin, V., Regis, J., Poupon, F., Pachot-Clouard, M., Le Bihan, D., and Bloch, I. 1998. Regularization of mr diffusion tensor maps for tracking brain white matter bundles. In W.M. Wells, A. Colchester, and S. Delp (Ed.), *Medical Image Computing and Computer-Assisted Intervention-MICCAI'98*, Cambridge, MA, USA, vol. 1496 in Lecture Notes in Computer Science. Springer: Berlin, pp. 489–498.

Proesmans, M., Pauwels, E., and Van Gool, L. 1994. *Coupled Geometry-Driven Diffusion Equations for Low-Level Vision Geometry-Driven Diffusion in Computer Vision*, B.M. ter Haar Romeny (Ed.). Kluwer Academic Publishers: Boston, MA, pp. 191–228.

RealviZ. 1999. Web-site: http://www.realviz.com.

Rudin, L. and Osher, S. 1994. Total variation based image restoration with free local constraints. In *Proceedings of the International Conference on Image Procedings*, vol. I, pp. 31–35.

Rudin, L., Osher, S., and Fatemi, E. 1992. Nonlinear total variation based noise removal algorithms. *Physica* D, 60:259–268.

Sapiro, G. 1997. Color snakes. *Computer Vision and Image Understanding*, 68(2).

Sapiro, G. 1996. Vector-valued active contours. In *Proceedings of the International Conference on Computer Vision and Pattern Recognition*, San Francisco, CA. IEEE, pp. 680–685.

Sapiro, G. 2001. *Geometric Partial Differential Equations and Image Analysis*. Cambridge University Press.

Sapiro, G. and Ringach, D.L. 1996. Anisotropic diffusion of multivalued images with applications to color filtering. *IEEE Transactions on Image Processing*, 5(11):1582–1585.

Shah, J. 1996. A common framework for curve evolution, segmentation and anisotropic diffusion. In *International Conference on Computer Vision and Pattern Recognition*.

SHFJ CEA. 2000. Web page, *http://wwwdsv.cea.fr/thema/shfj/*.

Sochen, N., Kimmel, R., and Malladi, R. 1997. From high energy

physics to low level vision. In *Scale-Space Theories in Computer Vision*. pp. 236–247.

Sternberg, P. 1991. Vector-valued local minimizers of nonconvex variational problems. *Rocky Mt. J. Math.*, 21(2):799–807.

Strong, D.M. and Chan, T.F. 1996a. Relation of regularization parameter and scale in total variation based image denoising. In *Proc. IEEE Workshop on Mathematical Methods in Biomedical Image Analysis*.

Strong, D.M. and Chan, T.F. 1996b. Spatially and scale adaptive total variation based regularization and anisotropic diffusion in image processing. UCLA, Technical Report 46.

Tang, B., Sapiro, G., and Caselles, V. 2000. Diffusion of general data on non-flat manifolds via harmonic maps theory: The direction diffusion case. *The International Journal of Computer Vision*, 36(2):149–161.

Teboul, S., Blanc-Féraud, L., Aubert, G., and Barlaud, M. 1998. Variational approach for edge-preserving regularization using coupled PDE's. *IEEE Transaction on Image Processing*, Special Issue on PDE based Image Processing, 7(3):387–397.

ter Haar Romeny, B.M. 1994. *Geometry-Driven Diffusion in Computer Vision*. Computational Imaging and Vision. Kluwer Academic Publishers: Boston, MA.

Tikhonov, A.N. 1963. Regularization of incorrectly posed problems. *Soviet. Math. Dokl.*, 4:1624–1627.

Tschumperlé, D. and Deriche, R. 2001a. Constrained and unconstrained pde's for vector image restoration. In *Proceedings of the 10th Scandinavian Conference on Image Analysis*, Ivar Austvoll, (Ed.), Bergen, Norway, pp. 153–160.

Tschumperlé, D. and Deriche, R. 2001b. Diffusion tensor regularization with constraints preservation. In *IEEE Computer Society Conference on Computer Vision and Pattern Recognition*, Kauai Marriott, Hawaii.

Tschumperlé, D. and Deriche, R. 2001c. Regularization of orthonormal vector sets using coupled PDE's. In *IEEE Workshop on Variational and Level Set Methods*, Vancouver, Canada, pp. 3–10.

Tschumperlé, D. and Deriche, R. 2002. Diffusion pde's on vector-valued images: Local approach and geometric viewpoint. *IEEE Signal Processing Magazine*.

Vemuri, B., Chen, Y., Rao, M., McGraw, T., Mareci, T., and Wang, Z. 2001. Fiber tract mapping from diffusion tensor mri. In *1st IEEE Workshop on Variational and Level Set Methods in Computer Vision (VLSM'01)*.

Vese, L.A. and Osher, S. 2002. Numerical methods for pharmonic flows and applications to image processing. In *SIAM 50th Anniversary and Annual Meeting*.

Weickert, J. 1997. A review of nonlinear diffusion of filtering. In *Scale-Space Theory in Computer Vision*, vol. 1252 of Lecture Notes in Comp. Science. Springer; Berlin, pp. 3–28. Invited paper.

Weickert, J. 1998. *Anisotropic Diffusion in Image Processing*. Teubner-Verlag; Stuttgart.

Weickert, J. 1999. Linear scale space has first been proposed in Japan. *Journal of Mathematical Imaging and Vision*, 10(3):237–252.

Weickert, J. and Schnörr, C. 2001. A theoretical framework for convex regularizers in pde-based computation of image motion. *The International Journal of Computer Vision*, 45(3):245–264.

You, Y.L., Kaveh, M., Xu, W.Y., and Tannenbaum, A. 1994. Analysis and Design of Anisotropic Diffusion for Image Processing. In *Proceedings of the International Conference on Image Processing*, vol. II, pp. 497–501.